Periodic Graph Transformers for Crystal Material Property Prediction

Anonymous Author(s)
Affiliation
Address
email

Abstract

We consider representation learning on periodic graphs encoding crystal materials. Different from regular graphs, periodic graphs consist of a minimum unit cell repeating itself on a regular lattice in 3D space. How to effectively encode these periodic structures poses unique challenges not present in regular graph representation learning. In addition to being E(3) invariant, periodic graph representations need to be periodic invariant. That is, the learned representations should be invariant to shifts of cell boundaries as they are artificially imposed. Furthermore, the periodic repeating patterns need to be captured explicitly as lattices of different sizes and orientations may correspond to different materials. In this work, we propose a transformer architecture, known as Matformer, for periodic graph representation learning. Our Matformer is designed to be invariant to periodicity and can capture repeating patterns explicitly. In particular, Matformer encodes periodic patterns by efficient use of geometric distances between the same atoms in neighboring cells. Experimental results on multiple common benchmark datasets show that our Matformer outperforms baseline methods consistently. In addition, our results demonstrate the importance of periodic invariance and explicit repeating pattern encoding for crystal representation learning.

1 Introduction

Crystal material property prediction is important for the discovery of new materials with desirable properties [35, 32-34, 45, 47, 38, 3, 31, 4]. Different from molecules and proteins [13, 46, 39, 7, 44, 24, 41], which are commonly represented as graphs [42, 27, 10, 11, 23, 25], crystals consist of a minimum unit cell repeating itself on a regular lattice in 3D space. Thus, crystals are naturally represented as periodic graphs. A key challenge of crystal material property prediction lies in how to effectively encode periodic structures that are not present in regular molecular graph representations [8, 1, 18, 38, 21, 20, 29, 22, 36, 15]. Specifically, periodic graphs of crystals require unique periodic invariance. Periodic invariance has two facets; those are, the learned representations should be invariant to both the scaling up of the minimum repeatable unit cells and shifts of periodic boundaries. Although the former has been considered in Xie et al. [47, 48], the later is rarely identified explicitly and sometimes not considered by previous studies [47, 3, 43, 38, 4, 48, 31, 49]. Furthermore, the repeating patterns of periodic graphs should be captured explicitly. Given a fixed minimum unit cell structure, lattices of different sizes and orientations may correspond to different materials. Without such periodic patterns, the infinite structures of crystals may not be represented accurately. However, the explicit encoding of periodic patterns is not explored in previous studies [47, 3, 38, 4, 31].

In this work, we propose to tackle periodic graph representation learning by incorporating both periodic invariance and periodic pattern encoding. We propose a periodic graph transformer, known as Matformer, that is periodic invariant and can capture periodic repeating patterns explicitly for crystal

Submitted to 36th Conference on Neural Information Processing Systems (NeurIPS 2022). Do not distribute.

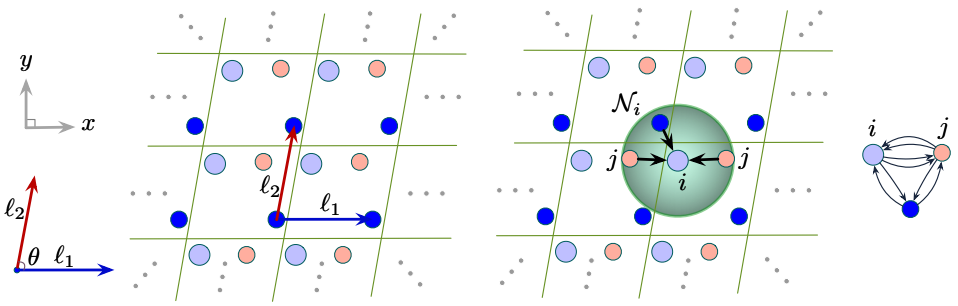

(a) (b) (c)

Figure 1: Illustrations of periodic patterns and the multi-edge graph construction method. Green lines are artificial boundaries to form one possible unit cell that repeats in infinite space for the given crystal. (a). An illustration of periodic patterns in 2D space. We use blue and red arrows to show how the blue atom repeats itself along ℓ_1 and ℓ_2. We show a general case in nature that ℓ_1 and ℓ_2 are not orthogonal. In this specific example, θ is less than $\frac{\pi}{2}$. (b) and (c). Illustrations of the multi-edge graph construction method and the constructed graph. The green circle shows atom i's neighborhood $\mathcal{N}_i$, and black arrows are edges from atom i's neighbors to itself. As atom j repeats twice within i's neighborhood in this example, the multi-edge graph construction method builds two edges from atom j to atom i. The crystals are 3D structures in practice, and we use illustrations in 2D for simplicity.

representation learning. Matformer achieves periodic invariance through two uniquely designed graph construction methods. It further encodes periodic patterns by efficient use of geometric distances between the same atoms in neighboring cells, thereby capturing the lattice size and orientation of a given crystal. We conduct experiments on two commonly used material benchmark datasets, including the Materials Project [14] and Jarvis [6]. Results show that Matformer outperforms baseline methods consistently on various tasks. In addition, our results demonstrate the importance of both periodic invariance and periodic pattern encoding for crystal representation learning.

2 Background

Crystal property prediction. Given a crystal represented as $(\mathbf{A}, \mathbf{P}, \mathbf{L})$, crystal property prediction aims to predict a target property value y, which is either real as $y \in \mathbb{R}$ or categorical as $y \in \mathbb{N}$ for regression or classification task. Specifically, a crystal is represented as a unit cell with periodic patterns. A unit cell is a minimum repeatable structure for the given crystal, and it can be described by matrices $\mathbf{A}$ and $\mathbf{P}$. $\mathbf{A} = [\boldsymbol{a}_1, \boldsymbol{a}_2, \cdots, \boldsymbol{a}_n]^T \in \mathbb{R}^{n \times d_a}$ is the atom feature matrix, where $\boldsymbol{a}_i \in \mathbb{R}^{d_a}$ is the d_a-dimensional feature vector for atom i in the unit cell. $\mathbf{P} = [\boldsymbol{p}_1, \boldsymbol{p}_2, \cdots, \boldsymbol{p}_n]^T \in \mathbb{R}^{n \times 3}$ is the position matrix, where $\boldsymbol{p}_i \in \mathbb{R}^3$ contains the Cartesian coordinates for atom i in 3D space. To further encode periodic patterns, an additional lattice matrix $\mathbf{L} = [\boldsymbol{\ell}_1, \boldsymbol{\ell}_2, \boldsymbol{\ell}_3]^T \in \mathbb{R}^{3 \times 3}$ is used to describe how a unit cell repeats itself in three directions, including $\boldsymbol{\ell}_1, \boldsymbol{\ell}_2$, and $\boldsymbol{\ell}_3$. We show a 2D case of periodic patterns for easy illustration in Fig. 1 (a). Note that crystals usually possess irregular shapes in practice. Hence, $\boldsymbol{\ell}_1$, $\boldsymbol{\ell}_2$, and $\boldsymbol{\ell}_3$ are not always orthogonal in 3D space. Formally, given a crystal representation $(\mathbf{A}, \mathbf{P}, \mathbf{L})$, the infinite crystal structure can be represented as

$$\begin{aligned} \hat{\mathbf{P}} =& \{\hat{\boldsymbol{p}}_i | \hat{\boldsymbol{p}}_i = \boldsymbol{p}_i + k_1\boldsymbol{\ell}_1 + k_2\boldsymbol{\ell}_2 + k_3\boldsymbol{\ell}_3,\ k_1, k_2, k_3 \in \mathbb{Z}, i \in \mathbb{Z}, 1 \leq i \leq n\}, \\ \hat{\mathbf{A}} =& \{\hat{\boldsymbol{a}}_i | \hat{\boldsymbol{a}}_i = \boldsymbol{a}_i, i \in \mathbb{Z}, 1 \leq i \leq n\}. \end{aligned} \tag{1}$$

Here, set $\hat{\mathbf{P}}$ contains all possible positions for each atom i, and set $\hat{\mathbf{A}}$ contains the corresponding atom feature vector for each atom i.

Multi-edge graph construction for crystals. The multi-edge graph construction proposed by Xie and Grossman [47] aims to capture atom interactions across cell boundaries, which are imposed artificially. In a regular molecular graph, a node corresponds to a single atom. In contrast, in a multi-edge graph, node i represents atom i and all its duplicates in the infinite 3D space. Apparently, node i contains the atom features vector $\boldsymbol{a}_i$ and all positions in the set $\{\hat{\boldsymbol{p}}_i | \hat{\boldsymbol{p}}_i = \boldsymbol{p}_i + k_1\boldsymbol{\ell}_1 + k_2\boldsymbol{\ell}_2 + k_3\boldsymbol{\ell}_3,\ k_1, k_2, k_3 \in \mathbb{Z}\}$, which is a subset of the infinite set $\hat{\mathbf{P}}$ defined in Eq. 1. Formally, the multi-edge graph construction method builds edges between nodes as follows. Given a prefixed radius $r \in \mathbb{R}$, if there exists any 3-tuple $(k_1^{'}, k_2^{'}, k_3^{'})$, where $k_1^{'}, k_2^{'}, k_3^{'} \in \mathbb{R}$, such that the Euclidean distance $d_{ji}^{'} \in \mathbb{R}$ satisfies

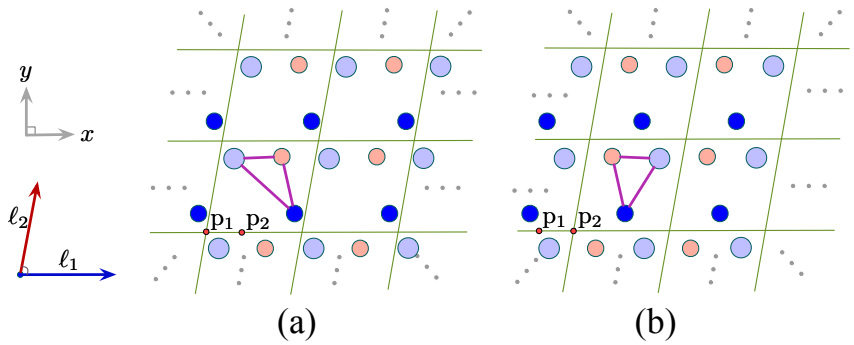

Figure 2: Illustration of periodic invariance. Green lines are artificial boundaries to form possible unit cells that repeat in infinite space. Purple lines are the edges between nodes inside a unit cell. Red points are the corner points of the unit cells. For example, p_1 and p_2 are for unit cells in (a) and (b), respectively. (a) and (b) show different unit cells describing the same crystal, caused by shifting the period boundaries along x axis from p_1 to p_2. By comparing (a) and (b), we show a graph construction method based on pairwise distances within the unit cell that breaks periodic invariance.

$d_{ji}^{'} = ||\boldsymbol{p}_j + k_1^{'}\boldsymbol{\ell}_1 + k_2^{'}\boldsymbol{\ell}_2 + k_3^{'}\boldsymbol{\ell}_3 - \boldsymbol{p}_i||_2 \leq r$, an edge is built from j to i with the initial edge feature $d_{ji}^{'}$. An example of the edge construction is shown in Fig. 1 (b). Intuitively, if there exist m positions of node j within the radius of the center node i, this method builds m edges from node j to node i. By considering all possible positions of every node within a predefined radius in 3D space, the multi-edge graph construction method can in essence capture atom interactions across cell boundaries. This graph construction method has been widely used in many following up studies [37, 31, 3, 38, 4].

3 The proposed Matformer

Different from molecular graphs, crystal graphs consist of a minimum unit cell repeating itself on a regular lattice in 3D space. When encoding such periodic structures, unique challenges lie in periodic invariance and periodic pattern encoding. In this section, we first propose to formally define periodic invariance and periodic pattern encoding. We then provide analyses to reveal the importance of these two considerations for the representation learning of periodic graphs encoding crystal materials. Finally, we present Matformer, a transformer architecture for periodic graph representation learning. It can be seen Matformer is invariant to periodicity and can capture repeating patterns explicitly.

3.1 Periodic invariance for crystals

Periodic invariance is proposed based on E(3) invariance for a unit cell. Hence, we first provide the formal definition of unit cell E(3) invariance as below.

Definition 1 (Unit Cell E(3) Invariance)**.** *A function $f : (\mathbf{A}, \mathbf{P}, \mathbf{L}) \rightarrow \mathcal{X}$ is unit cell E(3) invariant such that for all $Q \in \mathbb{R}^{3\times3}, |Q| = \pm1$ and $b \in \mathbb{R}^3$, we have $f(\mathbf{A}, \mathbf{P}, \mathbf{L}) = f(\mathbf{A}, Q\mathbf{P} + b, Q\mathbf{L})$, where Q is rotation and reflection transformations, and b is translation transformations in 3D space.*

Intuitively, unit cell E(3) invariance shows that the structure of a cell remains the same when either applying rotations and reflections to position matrix $\mathbf{P}$ and lattice matrix $\mathbf{L}$ together, or applying translations to $\mathbf{P}$ only.

In addition to unit cell E(3) invariance, periodic invariance is also shown necessary for generating valid crystal representations. Specifically, when the lattice matrix $\mathbf{L} = [\boldsymbol{\ell}_1, \boldsymbol{\ell}_2, \boldsymbol{\ell}_3]^T \in \mathbb{R}^{3\times3}$ is fixed for a crystal, we can still obtain different position matrices $\mathbf{P} \in \mathbb{R}^{n\times3}$ and different unit cell structures by shifting the period boundaries. As shown in Fig. 2 (a) and (b), the formed unit cell structures are different for the same crystal by shifting period boundaries. To this end, we further introduce periodic invariance, which shows that when the periodic boundaries are shifted or scaled up, the periodic invariant representation should remain the same. Formally, based on Sec. 2, we further define a function $\Phi : (\hat{\mathbf{A}}, \hat{\mathbf{P}}, \mathbf{L}, \mathrm{p}) \rightarrow (\mathbf{A}, \mathbf{P})$ simulating how to form different unit cells from a given infinite crystal structure. For an infinite crystal structure represented as $(\hat{\mathbf{A}}, \hat{\mathbf{P}})$, Φ uses a corner point p and shape matrix $\mathbf{L}$ to form a unit cell represented as $(\mathbf{A}, \mathbf{P})$. In addition, we use $\boldsymbol{\alpha} \in \mathbb{N}_+^3$ to indicate

the scaling up of a repeating unit cell formed by periodic boundaries. Then the formal definition of periodic invariance is provided as below.

Definition 2 (Periodic Invariance)**.** *A unit cell E(3) invariant function* $f : (\mathbf{A}, \mathbf{P}, \mathbf{L}) \to \mathcal{X}$ *is periodic invariant if* $f(\mathbf{A}, \mathbf{P}, \mathbf{L}) = f(\Phi(\hat{\mathbf{A}}, \hat{\mathbf{P}}, \boldsymbol{\alpha}\mathbf{L}, \mathrm{p}), \boldsymbol{\alpha}\mathbf{L})$ *holds for all* $\mathrm{p} \in \mathbb{R}^3$ *and* $\boldsymbol{\alpha} \in \mathbb{N}_+^3$.

Significance of periodic invariance. Breaking periodic invariance will result in different crystal graphs for the same crystal. In Fig. 2 (a) and (b), we show a graph construction method that breaks periodic invariance. This method is employed by a transformer-based model, known as Graphormer [49], for learning from adsorbates and catalyst surface systems [2]. In particular, Graphormer first uses radius to include all the atoms of interest in nearby cells and then builds a fully connected graph. A detailed illustration is shown in Fig. 5 in Appendix. A.1. Based on the formal definition of periodic invariance, in this study, we aim to integrate such an important component in our Matformer. By doing this, our model is able to construct a distinct crystal graph for a given crystal structure, resulting in a more informative and discriminative crystal learning scheme.

3.2 Periodic pattern encoding

As introduced in Sec. 2, $\mathbf{L} = [\boldsymbol{\ell}_1, \boldsymbol{\ell}_2, \boldsymbol{\ell}_3]^T \in \mathbb{R}^{3\times 3}$ containing periodic patterns is another key component to describe crystal structures. Essentially, periodic patterns show how the minimum repeatable structure $(\mathbf{A}, \mathbf{P})$ expands itself in infinite 3D space. Without such periodic pattern encoding in $\mathbf{L}$, crystal structures are treated as finite structures similar to molecules. As shown in Fig. 3, the widely used multi-edge graph construction method [47, 3, 38, 37, 4] only captures local interactions among atoms but ignores the important periodic patterns. However, such periodic repeating patterns need to be captured explicitly, as lattices of different sizes and orientations may correspond to different materials. Hence, To better represent the infinite structures of crystals, we argue that the periodic patterns $\mathbf{L} \in \mathbb{R}^{3\times 3}$ should be explicitly taken into consideration in crystal learning.

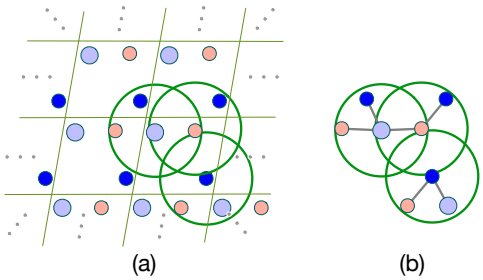

Figure 3: Illustration that periodic patterns are not encoded in a multi-edge graph. The green circles denote the prefixed radius, and the grey lines are the captured topology information by the multi-edge graph construction. We use three radius circles because there are three atoms in a unit cell. (a). Illustration of the multi-edge graph construction. (b). Illustration that the multi-edge graph method only captures local geometric information but ignores periodic patterns for the infinite crystal structure.

3.3 The proposed graph construction methods

In this section, we introduce the proposed graph construction methods for Matformer. Our methods effectively integrate the above two components for accurate crystal representation learning.

Invariant crystal graph construction. We consider two crystal graph construction methods, including radius-based graph construction and fully connected graph construction. Both of them satisfy periodic invariance, and mathematical proofs can be found in Appendix. A.2. In Fig. 2, we show by example that treating atoms as single nodes breaks periodic invariance. Instead, in our methods, we follow the fashion introduced in Sec. 2 to treat node i in a constructed graph as atom i and all its repeated duplicates in infinite 3D space.

We use the multi-edge graph construction [47] introduced in Sec. 2 as an alternative crystal graph construction method. Note that although the multi-edge graph construction satisfies periodic invariance as in Fig. 4 (a), several existing works [47, 31] do not follow the settings exactly thus breaking periodic invariance. Within the given radius shown in Fig. 4 (a), these studies form the neighborhood of node i by selecting t nearest neighbors ranked by geometric distances. If there exist several different atoms with the same distance to node i, there is no deterministic way to select from them, as shown in Fig. 6 in Appendix. A.1. As a result, periodic invariance cannot be guaranteed.

Given the fully-connected fashion employed in Graphormer has achieved impressive performance on molecular learning, we further propose another graph construction method for Matformer, known as the fully connected graph construction. This method uses a different strategy to determine neighbors

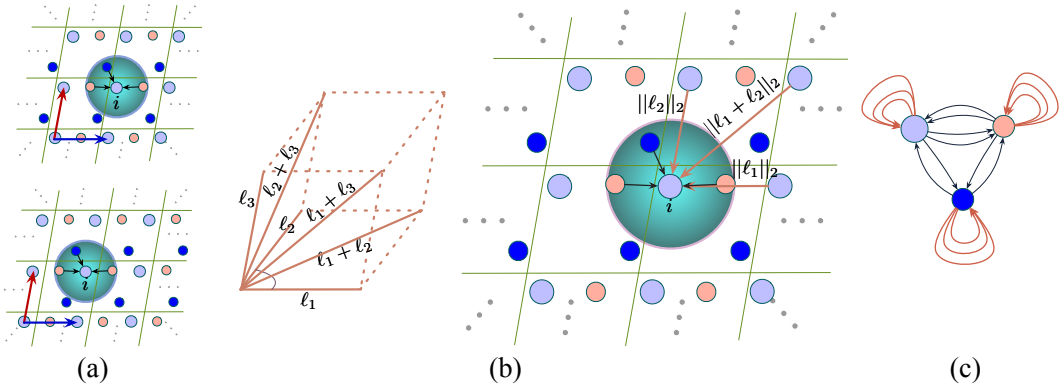

Figure 4: Illustrations of the used radius-based graph construction method and the proposed periodic pattern encoding for Matformer. Each green circle shows neighborhood of node i with a prefixed radius. Black arrows are the formed edges by radius-based graph construction and brown arrows are self-connecting edges. (a). Illustration that the used radius-based graph construction satisfies periodic invariance. (b). Illustration of periodic pattern encoding using self-connecting edges. On the left, we show the designed self-connecting edges to encode the lattice matrix $\mathbf{L} = [\boldsymbol{\ell}_1, \boldsymbol{\ell}_2, \boldsymbol{\ell}_3]^T \in \mathbb{R}^{3\times3}$ in 3D space. We design six self-connecting edges $||\ell_1||_2$, $||\ell_2||_2$, $||\ell_3||_2$, $||\ell_1+\ell_2||_2$, $||\ell_1+\ell_3||_2$, $||\ell_2+\ell_3||_2$. The geometric shape of $\mathbf{L}$ can be determined by these six edges. On the right, we show the added self-connecting edges in 2D space for easy illustration. We use $||\ell_1||_2$, $||\ell_2||_2$, and $||\ell_1+\ell_2||_2$ to encode periodic patterns in this 2D case. (c). Illustration of the constructed graph with periodic pattern encoding for the above 2D case.

for each center node. Specifically, for node i and j, it builds edges for the entries corresponding to the t smallest distances in $\{d_{ij} | d_{ij} = ||\boldsymbol{p}_i - \boldsymbol{p}_j + k_1^{'}\boldsymbol{\ell}_1 + k_2^{'}\boldsymbol{\ell}_2 + k_3^{'}\boldsymbol{\ell}_3||_2,\ k_1^{'}, k_2^{'}, k_3^{'} \in \mathbb{Z}\}$. It can be seen every pair i and j is connected in the constructed graph and there are t edges between them.

Overall, the used multi-edge graph construction and proposed fully-connected graph construction both satisfy the important periodic invariance. Particularly, they possess great flexibility to be used in future studies for crystal learning. In this study, we employ both methods as part of our proposed Matformer, and in main experiments, the radius-based method is used due to better empirical performance.

Periodic pattern encoding with self-connecting edges. In this study, we propose to encode the important $\mathbf{L} = [\boldsymbol{\ell}_1, \boldsymbol{\ell}_2, \boldsymbol{\ell}_3]^T \in \mathbb{R}^{3\times3}$ into crystal graphs by adding self-connecting edges. As mentioned in Sec. 3.2, periodic patterns describe sizes and orientations of lattices of a crystal structure, eventually determining the properties of this crystal. A natural step for encoding such repeating periodic patterns is to consider the relative positions between an atom and its nearby repeated duplicates. Formally, given an atom i with position $\boldsymbol{p}_i$ and $\mathbf{L} = [\boldsymbol{\ell}_1, \boldsymbol{\ell}_2, \boldsymbol{\ell}_3]^T \in \mathbb{R}^{3\times3}$, we need to encode the atom's three nearby duplicates with positions $\boldsymbol{p}_i + \boldsymbol{\ell_1}$, $\boldsymbol{p}_i + \boldsymbol{\ell_2}$, and $\boldsymbol{p}_i + \boldsymbol{\ell_3}$. It is widely known that a direction vector $\boldsymbol{\ell}_i$ is determined by both its length $||\boldsymbol{\ell}_i||_2$ and orientation. Essentially, $||\boldsymbol{\ell}_i||_2$ indicates the geometric distance between atom i and its corresponding duplicate. However, the computing of orientation information, such as angles, usually induces high complexity. Hence, it is not practical to encode such orientation information into transformer architectures. To this end, we propose to use geometric distances solely to implicitly consider the orientation information.

Specifically, we use additional distances to determine angles between any two direction vectors in $\mathbf{L}$. For example, the angle between $\boldsymbol{\ell}_1$ and $\boldsymbol{\ell}_2$ can be easily computed by $||\boldsymbol{\ell}_1||_2$, $||\boldsymbol{\ell}_2||_2$, and an additional distance $||\boldsymbol{\ell}_1 + \boldsymbol{\ell}_2||_2$. Hence, based on these three distances, we can determine lengths of $\boldsymbol{\ell}_1$ and $\boldsymbol{\ell}_2$, and the relative orientation between them. Extensively, we use six geometric distances, including $||\boldsymbol{\ell}_1||_2$, $||\boldsymbol{\ell}_2||_2$, $||\boldsymbol{\ell}_3||_2$, $||\boldsymbol{\ell}_1 + \boldsymbol{\ell}_2||_2$, $||\boldsymbol{\ell}_2 + \boldsymbol{\ell}_3||_2$, and $||\boldsymbol{\ell}_1 + \boldsymbol{\ell}_3||_2$ in our study, as shown in Fig. 4 (b). By doing this, the length of each direction vector and the angle between any two direction vectors can all be determined. As a result, the shape formed by lattice matrix $\mathbf{L}$ is then fixed. Overall, we build the aforementioned six geometric distances as six self-connecting edges for node i. By doing this, our model is capable of encoding periodic patterns in $\mathbf{L}$ completely, resulting in a more accurate crystal representation learning scheme. Importantly, our approach also guarantees periodic invariance. This is because the pairwise distances do not change when the periodic boundaries are shifted.

Overall, the graph construction for Matformer consists of two necessary stages, including invariant graph construction and periodic pattern encoding. For the first stage, we rigorously prove that the multi-edge graph construction satisfies periodic invariance and show that several previous works [47, 31] break periodic invariance using a different neighbor selection strategy. Additionally, we propose a fully-connected crystal graph construction method satisfying periodic invariance, and the method could be used in future studies for crystal representation learning. For the second stage, we naturally encode periodic patterns into constructed graphs by adding self-connecting edges without breaking periodic invariance. A constructed graph in 2D case is shown in Fig. 4 (c).

3.4 Message passing scheme

Building on constructed graphs introduced in Sec. 3.3, we propose our message passing scheme for Matformer. Formally, we denote a constructed crystal graph as $G = (\mathbf{A}, \mathbf{E})$. Here, each $\boldsymbol{a}_i \in \mathbf{A}$ is the d_a-dimensional feature vector for atom i, as introduced in Sec. 2. Particularly, $\boldsymbol{e}_{ij}^h \in \mathbf{E}$ is d_e-dimensional feature vector for the h-th edge between nodes i and j. We follow the regular attention mechanism that computes query, key, and value [28, 26]. Our proposed message passing scheme is composed of three steps; those are, edge-wise attention coefficients computing, edge-wise value message computing, and node updating. Formally, we let $\boldsymbol{f}_i^\star$ denote the input feature vector of node i for the ℓ-th layer of Matformer. The message passing scheme of the ℓ-th layer is described as below.

In the first step, $\boldsymbol{q}_{ij}^h$, $\boldsymbol{k}_{ij}^h$ and $\boldsymbol{\alpha}_{ij}^h$ for the h-th edge between i and j are computed as

$$\begin{aligned} \boldsymbol{q}_i =& \mathrm{LN}_Q(\boldsymbol{f}_i^\star),\ \boldsymbol{k}_i = \mathrm{LN}_K(\boldsymbol{f}_i^\star),\ \boldsymbol{k}_j = \mathrm{LN}_K(\boldsymbol{f}_j^\star),\ \boldsymbol{e}_{ij}^{h'} = \mathrm{LN}_E(\boldsymbol{e}_{ij}^h), \\ \boldsymbol{q}_{ij}^h =& (\boldsymbol{q}_i|\boldsymbol{q}_i|\boldsymbol{q}_i),\ \ \boldsymbol{k}_{ij}^h = (\boldsymbol{k}_i|\boldsymbol{k}_j|\boldsymbol{e}_{ij}^{h'}),\ \ \boldsymbol{\alpha}_{ij}^h = \frac{\boldsymbol{q}_{ij}^h \circ \boldsymbol{k}_{ij}^h}{\sqrt{d_{\boldsymbol{k}_{ij}^h}}}, \end{aligned} \tag{2}$$

where LN_Q, LN_K, and LN_E denote the linear transformations to compute query, key, and edge embedding in ℓ-th layer, respectively. $\boldsymbol{e}_{ij}^{h'}$ is the intermediate output for $\boldsymbol{e}_{ij}^h$. We use $\circ$ and $|$ to denote Hadamard Product and concatenation. Particularly, we omit the softmax to enhance the model's capability to distinguish nodes with different degrees, and to make the whole network more efficient.

After obtaining the attention coefficients $\boldsymbol{\alpha}_{ij}^h$, in the second step, we compute $\boldsymbol{m}_{ij}^h$ that is the message of edge $\boldsymbol{e}_{ij}^h$ as

$$\boldsymbol{v}_i = \mathrm{LN}_V(\boldsymbol{f}_i^\star),\ \boldsymbol{v}_j = \mathrm{LN}_V(\boldsymbol{f}_j^\star), \boldsymbol{m}_{ij}^h = \mathrm{sigmoid}(\mathrm{LNorm}(\boldsymbol{\alpha}_{ij}^h)) \circ \mathrm{LN}_{\mathrm{update}}(\boldsymbol{v}_i|\boldsymbol{v}_j|\boldsymbol{e}_{ij}^{h'}), \tag{3}$$

where LN_V and $\mathrm{LN}_{\mathrm{update}}$ are the linear transformations to compute value and the updated message, and LNorm denotes the layer normalization operation. In particular, we apply sigmoid and Layer normalization to $\boldsymbol{\alpha}_{ij}^h$ to stabilize the training.

Finally, in the third step, we compute node i's feature vector $\boldsymbol{f}_i$. Specifically, we first obtain message $\boldsymbol{m}_i$ by aggregating information from node i's neighborhood over multiple edges, then achieve $\boldsymbol{f}_i$ as

$$\boldsymbol{m}_i = \sum_{j \in \mathcal{N}_i} \sum_h \mathrm{LNorm}(\mathrm{LN}_{\mathrm{msg}}(\boldsymbol{m}_{ij}^h)),\ \boldsymbol{f}_i = \mathrm{LN}_{\mathrm{fea}}(\boldsymbol{f}_i^\star) + \sigma(\mathrm{BN}(\boldsymbol{m}_i)), \tag{4}$$

where σ is the used activation function, and BN indicates batch normalization. In addition, $\mathrm{LN}_{\mathrm{msg}}$ and $\mathrm{LN}_{\mathrm{fea}}$ are linear transformations to update the messages on edges and the old atom features.

Graphormer represents an effective transformer variant for molecular graph learning. The differences between Graphormer and the proposed Matformer lie in both graph construction and message passing scheme. Firstly, Graphormer treats every atom as a single node. Also, as there is only one geometric distance between node i and j in 3D space, a single edge will be built between them. Apparently, Graphormer breaks periodic invariance, as mentioned in Sec. 3.1. However, our proposed Matformer satisfies periodic invariance by employing the crystal graph construction methods described in Sec. 3.3. For the message passing, Graphormer uses the node-wise attention and encodes pairwise distances as attention bias. It cannot work properly on multi-edge graphs for crystals. While Matformer is specifically designed for multi-edge crystal graphs by performing edge-wise attention and encoding geometric information into edge-wise messages, as described above. The detailed architecture of our Matformer is shown in Fig. 7 in Appendix.

4 Related work

Crystal property prediction. Several existing methods [43, 16, 17, 12] model crystals as chemical formulas and employ sequence models to process such sequential formulas. Other studies [47, 37, 31, 3, 38, 4] consider 3D structures of crystals and formulate crystals as 3D graphs, then apply GNNs to learn from crystal graphs. As crystals are essentially periodically repeated structures, the graph construction needs to consider periodic invariance and periodic pattern encoding. There are limited efforts to identify these two unique components. As an early work, CGCNN [47] proposes to capture atom interactions across artificial cell boundaries by using multi-edge graphs described in Sec. 2. The multi-edge graph satisfies periodic invariance as described in Sec. 3.1, but fails to consider the important periodic patterns, as described in Sec. 3.2. The multi-edge graph construction method is widely used in the following studies [37, 31, 3, 38, 4]. Based on the constructed crystal graphs, many GNN variants have been proposed for effective crystal representation learning [47, 37, 31, 3, 38, 4]. Recently, ALIGNN [4] achieves the state-of-the-art performance on two major material datasets. It uses angle information in the message passing procedure to generate more informative and discriminative representations. However, the use of angles introduces excessive time complexity.

Geometric GNNs and graph transformer. Many efforts have been made to incorporate 3D geometric information in molecular learning. Exemplary studies include SchNet [38], DimeNet [21, 20], SphereNet [29], GemNet [22], etc. However, these methods are designed for molecules without periodic patterns. Recently, graph transformers [49, 9] using geometric information, e.g., Graphormer [49], have shown great potential on real-world graph data. However, Graphormer considers neither periodic invariance no periodic pattern encoding.

Differences with our method. To the best of our knowledge, periodic invariance and periodic pattern encoding described in Sec. 3 are rarely identified and explored in existing works for crystal property prediction. CGCNN [47] breaks periodic invariance on some corner cases because it uses twelve nearest neighbors determined only by distances as described in Sec. 3.3. In addition, previous methods including CGCNN [47], SchNet [38], MEGNET [3], CYATT [37], GATGNN [31], and ALIGNN [4], all fail to consider the important periodic pattern encoding as introduced in Sec. 3.2. For Graphormer [49], although it achieved remarkable success on the Open Catalyst Challenge [2], the employed graph construction method breaks periodic invariance when applied to crystals. Compared with Graphormer, Matformer is specifically designed for crystals considering both periodic invariance and periodic patterns. In addition, different from the node-wise attention used in Graphormer, our Matformer employs edge-wise attention and aggregates information from edges as in Sec. 3.4.

5 Experimental studies

5.1 Experimental setup

We conduct experiments on two material benchmark datasets, including The Materials Project [14] and JARVIS [6]. Baseline methods include CFID [5], CGCNN [47], SchNet [38], MEGNET [3], GATGNN [31], and ALIGNN [4]. Unless otherwise specified, for all the baseline methods, we

Table 1: Comparison between Matformer and other baselines in terms of test MAE on The Materials Project 2018.6.1 dataset. We show the results both from our retrained models and from referred papers to make the comparison clear and fair. Specifically, we retrain corresponding models by using exactly the same training, validation, and test sets as our Matformer for these four tasks. Results from original papers are shown in parentheses () on the right. '-' denotes no results are reported in referred papers. The best results are shown in **bold** and the second best results are shown with underlines.

	Formation Energy	Band Gap	Bulk Moduli	Shear Moduli
Method	eV/atom	eV	log(GPa)	log(GPa)
CGCNN [47]	0.031 (0.039)	0.292 (0.388)	0.047 (0.054)	0.077 (0.087)
SchNet [38]	0.033 (0.035)	0.345 (-)	0.066 (-)	0.099 (-)
MEGNET [3]	0.030 (0.028)	0.307 (0.33)	0.060 (0.050)	0.099 (0.079)
GATGNN [31]	0.033 (0.048)	0.280 (0.31)	0.045	0.075
ALIGNN [4]	0.022	0.218	0.051 (-)	0.078 (-)
Matformer	**0.021**	**0.211**	**0.043**	**0.073**

report the results taken from the referred papers or provided by original authors. All Matformer models are trained using the Adam optimizer [19] with weight decay [30] and one cycle learning rate scheduler [40]. We only slightly adjust learning rates from 0.001 and training epochs from 500 for different tasks. Detailed Matformer configurations for different tasks are provided in Appendix. A.3.

5.2 The Materials Project dataset

We first use The Materials Project-2018.6.1 dataset [3], which contains 69239 crystals, to evaluate Matformer. We notice that previous works [47, 38, 3, 31, 4] compare with each other either using datasets of different sizes, or using datasets with the same size but splitting the datasets with different random seeds. To make the comparison clear and fair, we retrain all corresponding models using exactly the same training, validation and test sets across all methods and report the results in Table. 1. To avoid confusion, we still put original results from referred papers in Table. 1 inside parentheses. In particular, for tasks of formation energy and band gap, we directly follow ALIGNN [4] and use the same training, validation, and test set, including 60000, 5000, and 4239 crystals, respectively. For tasks of Bulk Moduli and Shear Moduli, we follow GATGNN [31], the recent state-of-the-art method for these two tasks, and use the same training, validation, and test sets, including 4664, 393, and 393 crystals. In Shear Moduli, one validation sample is removed because of the negative GPa value. We either directly use the publicly available codes from the authors, or re-implement models based on their official codes and configurations to produce the results. Detailed configurations of these retrained models are provided in Appendix. A.4. The used metric is test MAE following previous studies [47, 38, 3, 31, 4].

It can be seen from Table. 1 that Matformer achieves the best performance on all tasks consistently by significant margins. Specifically, it reduces the formation energy by 4.5% of the second best model, which is a significant margin. Furthermore, for Bulk Moduli and Shear Moduli tasks with only 4664 training samples, Matformer achieves the best performances, indicating Matformer's adaptive ability to tasks of small training scales. The overall excellent performances for different tasks on The Materials Project reveal the effectiveness of our proposed crystal graph representations in Matformer.

5.3 JARVIS dataset

JARVIS is a newly released database proposed by Choudhary et al. [6]. For JARVIS dataset, we follow ALIGNN [4] and use the same training, validation, and test set. We evaluate our Matformer on five important crystal property tasks, including formation energy, bandgap(OPT), bandgap(MBJ), total energy, and Ehull. The training, validation, and test set contains 44578, 5572, and 5572 crystals for tasks of formation energy, total energy, and bandgap(OPT). The numbers are 44296, 5537, 5537 for Ehull, and 14537, 1817, 1817 for bandgap(MBJ). The used metric is test MAE. The results for all baselines are taken from ALIGNN [4].

The quantitative results for Jarvis are shown in Table. 3. Matformer outperforms the baseline methods significantly on all of these five tasks. Compared with ALIGNN, Matformer has stronger discriminative ability due to explicit encoding of periodic patterns. Specifically, Matformer reduces Jarvis Ehull by 0.012, which is 15.8% of ALIGNN. Furthermore, Matformer achieves the best performances for Bulk Moduli and Shear Moduli in the Mateirals Project with 4664 training samples, and Bandgap(MBJ) in JARVIS with 14537 training samples, indicating its adaptive ability to tasks of various data scales. Overall, the superior performances of our Matformer on various tasks of two common material benchmarks show effectiveness of periodic pattern encoding and great potential of our Matformer message passing layer for crystal graphs. In addition, compared with ALIGNN, the previous state-of-the-art method for crystal property prediction, our Matformer is more efficient. We evaluate the efficiency of Matformer by comparing with ALIGNN using JARVIS formation energy dataset. The mean time of ten runs for training and inference time, using corresponding best model configurations of ALIGNN and Matformer, is reported. And the total time is computed by Time/epoch $\times$ corresponding training epoch number, which is 300 for ALIGNN and 500 for Matformer. In Table. 2, we show that Matformer is three times faster than ALIGNN in total training time and near three times faster in inference time, for the whole test set.

Table 2: Efficiency comparison with ALIGNN on Jarvis formation energy. We show the training time per epoch, total training time and inference time.

Models	Time/epoch	Total	Inference
ALIGNN	327 s	27.3 h	156 s
Matformer	64 s	8.9 h	59 s

Table 3: Comparison between Matformer and other baselines in terms of test MAE on JARVIS dataset. The best results are shown in **bold** and the second best results are shown with underlines.

Method	Formation Energy eV/atom	Bandgap(OPT) eV	Total Energy eV/atom	Ehull eV	Bandgap(MBJ) eV
CFID [5]	0.14	0.30	0.24	0.22	0.53
CGCNN [47]	0.063	0.20	0.078	0.17	0.41
ALIGNN [4]	0.0331	0.142	0.037	0.076	0.31
Matformer	**0.0325**	**0.137**	**0.035**	**0.064**	**0.30**

5.4 Ablation study

In this section, we demonstrate the importance of periodic invariance and explicit repeating pattern encoding for crystal representation learning by ablation studies. We also evaluate the building blocks particularly designed for our Matformer. Specifically, we conduct experiments on JARVIS formation energy, and the test MAE is used as the quantitative evaluation metric.

Periodic invariant graph construction. We demonstrate the importance of periodic invariant graph construction by comparing radius multi-edge graph, denoted as Radius, with the graph construction method proposed by Graphormer, denoted as OCgraph. Note that the constructed crystal graphs by OCgraph are super large, containing more than n^2 edges, where n is the atom number in a cell. We adjust the Matformer configurations to train these large graphs on a single RTX A6000 GPU. We use same model and training configurations for these two graph construction methods. It can be seen from Table. 4 that when using OCgraph to our Matformer, the test MAE drops dramatically of 53% because of breaking periodic invariance, compared with radius-based multi-edge graphs used in Matformer.

Table 4: Ablation studies about periodic invariance and periodic pattern encoding. We use OCgraph to denote graph construction method of Graphormer. PI denotes periodic invariance and PE denotes periodic encoding.

Graph	PI	PE	layer	head	batch	Test MAE
OCgraph	×	×	3	1	32	0.0530
Radius w/o PE	✓	×	3	1	32	0.0348
Radius w/o PE	✓	×	5	4	64	0.0337
T-fully w PE	✓	✓	5	4	64	0.0402
Radius w PE	✓	✓	5	4	64	**0.0325**

Encoding of repeating patterns. We denote periodic pattern encoding as PE. In Table. 4, we show that omitting the periodic pattern encoding results in a significant drop of test MAE from 0.0325 to 0.0337, revealing the importance of periodic patterns for crystal representation learning.

Building blocks of Matformer. Firstly, in Table. 4, we compare two periodic invariant graph construction methods described in Sec. 3.3. We deonte fully connected graph with t smallest pairwise distances as T-fully, and we use $t = 3$. Results show that although both methods satisfy periodic invariance, Radius is better than T-fully. In addition, we evaluate the operation of sigmoid and normalization instead of softmax in our message passing, which is designed to capture the node degree information in multi-edge crystal graphs, described in Sec. 3.4. Compared with using softmax with scalar attention coefficient, denoted as Softmax-scalar, or softmax with vector attention coefficient, denoted as Softmax-vector, using sigmoid and normalization leading to significant performance improvement in terms of test MAE, justifying the effectiveness of this operation in Matformer message passing design, shown in Table. 5.

Table 5: Operation ablation study.

Operation	Test MAE
Softmax-scalar	0.0376
Softmax-vector	0.0347
Sigmoid and Norm	**0.0325**

6 Conclusion

In this work, we first propose to formally define periodic invariance and periodic pattern encoding for periodic graph learning. We then propose Matformer for periodic graph representation learning, which is invariant to periodicity and can capture repeating patterns explicitly. Experimental results on common benchmark datasets show that our Matformer outperforms baseline methods consistently. In addition, our results demonstrate the importance of periodic invariance and explicit periodic pattern encoding for crystal representation learning.

References

[1] Simon Batzner, Albert Musaelian, Lixin Sun, Mario Geiger, Jonathan P Mailoa, Mordechai Kornbluth, Nicola Molinari, Tess E Smidt, and Boris Kozinsky. E (3)-equivariant graph neural networks for data-efficient and accurate interatomic potentials. Nature Communications, 13(1): 1–11, 2022.

[2] Lowik Chanussot*, Abhishek Das*, Siddharth Goyal*, Thibaut Lavril*, Muhammed Shuaibi*, Morgane Riviere, Kevin Tran, Javier Heras-Domingo, Caleb Ho, Weihua Hu, Aini Palizhati, Anuroop Sriram, Brandon Wood, Junwoong Yoon, Devi Parikh, C. Lawrence Zitnick, and Zachary Ulissi. Open catalyst 2020 (oc20) dataset and community challenges. ACS Catalysis, 2021. doi: 10.1021/acscatal.0c04525.

[3] Chi Chen, Weike Ye, Yunxing Zuo, Chen Zheng, and Shyue Ping Ong. Graph networks as a universal machine learning framework for molecules and crystals. Chemistry of Materials, 31 (9):3564–3572, 2019.

[4] Kamal Choudhary and Brian DeCost. Atomistic line graph neural network for improved materials property predictions. npj Computational Materials, 7(1):1–8, 2021.

[5] Kamal Choudhary, Brian DeCost, and Francesca Tavazza. Machine learning with force-field-inspired descriptors for materials: Fast screening and mapping energy landscape. Physical review materials, 2(8):083801, 2018.

[6] Kamal Choudhary, Kevin F Garrity, Andrew CE Reid, Brian DeCost, Adam J Biacchi, Angela R Hight Walker, Zachary Trautt, Jason Hattrick-Simpers, A Gilad Kusne, Andrea Centrone, et al. The joint automated repository for various integrated simulations (jarvis) for data-driven materials design. npj Computational Materials, 6(1):1–13, 2020.

[7] Alex Fout, Jonathon Byrd, Basir Shariat, and Asa Ben-Hur. Protein interface prediction using graph convolutional networks. Advances in neural information processing systems, 30, 2017.

[8] Fabian Fuchs, Daniel Worrall, Volker Fischer, and Max Welling. Se (3)-transformers: 3d roto-translation equivariant attention networks. Advances in Neural Information Processing Systems, 33:1970–1981, 2020.

[9] Fabian Fuchs, Daniel Worrall, Volker Fischer, and Max Welling. Se (3)-transformers: 3d roto-translation equivariant attention networks. Advances in Neural Information Processing Systems, 33:1970–1981, 2020.

[10] Hongyang Gao and Shuiwang Ji. Graph u-nets. In international conference on machine learning, pages 2083–2092. PMLR, 2019.

[11] Hongyang Gao, Yi Liu, and Shuiwang Ji. Topology-aware graph pooling networks. IEEE Transactions on Pattern Analysis and Machine Intelligence, 43(12):4512–4518, 2021.

[12] Rhys EA Goodall and Alpha A Lee. Predicting materials properties without crystal structure: Deep representation learning from stoichiometry. Nature communications, 11(1):1–9, 2020.

[13] Marco Gori, Gabriele Monfardini, and Franco Scarselli. A new model for learning in graph domains. In Proceedings. 2005 IEEE international joint conference on neural networks, volume 2, pages 729–734, 2005.

[14] Anubhav Jain, Shyue Ping Ong, Geoffroy Hautier, Wei Chen, William Davidson Richards, Stephen Dacek, Shreyas Cholia, Dan Gunter, David Skinner, Gerbrand Ceder, et al. Commentary: The materials project: A materials genome approach to accelerating materials innovation. APL materials, 1(1):011002, 2013.

[15] Priyank Jaini, Lars Holdijk, and Max Welling. Learning equivariant energy based models with equivariant stein variational gradient descent. Advances in Neural Information Processing Systems, 34, 2021.

[16] Dipendra Jha, Logan Ward, Arindam Paul, Wei-keng Liao, Alok Choudhary, Chris Wolverton, and Ankit Agrawal. Elemnet: Deep learning the chemistry of materials from only elemental composition. Scientific reports, 8(1):1–13, 2018.

[17] Dipendra Jha, Logan Ward, Zijiang Yang, Christopher Wolverton, Ian Foster, Wei-keng Liao, Alok Choudhary, and Ankit Agrawal. Irnet: A general purpose deep residual regression framework for materials discovery. In Proceedings of the 25th ACM SIGKDD International Conference on Knowledge Discovery & Data Mining, pages 2385–2393, 2019.

[18] Nicolas Keriven and Gabriel Peyré. Universal invariant and equivariant graph neural networks. Advances in Neural Information Processing Systems, 32, 2019.

[19] Diederik P Kingma and Jimmy Ba. Adam: A method for stochastic optimization. In Proceedings of the 3rd International Conference on Learning Representations, 2015.

[20] Johannes Klicpera, Shankari Giri, Johannes T Margraf, and Stephan Günnemann. Fast and uncertainty-aware directional message passing for non-equilibrium molecules. arXiv preprint arXiv:2011.14115, 2020.

[21] Johannes Klicpera, Janek Groß, and Stephan Günnemann. Directional message passing for molecular graphs. iclr, 2020.

[22] Johannes Klicpera, Florian Becker, and Stephan Günnemann. Gemnet: Universal directional graph neural networks for molecules. In Advances in Neural Information Processing Systems, 2021.

[23] Meng Liu, Hongyang Gao, and Shuiwang Ji. Towards deeper graph neural networks. In Proceedings of the 26th ACM SIGKDD International Conference on Knowledge Discovery & Data Mining. ACM, 2020.

[24] Meng Liu, Youzhi Luo, Limei Wang, Yaochen Xie, Hao Yuan, Shurui Gui, Haiyang Yu, Zhao Xu, Jingtun Zhang, Yi Liu, et al. Dig: a turnkey library for diving into graph deep learning research. Journal of Machine Learning Research, 22(240):1–9, 2021.

[25] Meng Liu, Keqiang Yan, Bora Oztekin, and Shuiwang Ji. Graphebm: Molecular graph generation with energy-based models. arXiv preprint arXiv:2102.00546, 2021.

[26] Yi Liu and Shuiwang Ji. Cleftnet: Augmented deep learning for synaptic cleft detection from brain electron microscopy. IEEE Transactions on Medical Imaging, 40(12):3507–3518, 2021.

[27] Yi Liu, Hao Yuan, Lei Cai, and Shuiwang Ji. Deep learning of high-order interactions for protein interface prediction. In Proceedings of the 26th ACM SIGKDD international conference on knowledge discovery & data mining, pages 679–687, 2020.

[28] Yi Liu, Hao Yuan, Zhengyang Wang, and Shuiwang Ji. Global pixel transformers for virtual staining of microscopy images. IEEE Transactions on Medical Imaging, 39(6):2256–2266, 2020.

[29] Yi Liu, Limei Wang, Meng Liu, Yuchao Lin, Xuan Zhang, Bora Oztekin, and Shuiwang Ji. Spherical message passing for 3d molecular graphs. In International Conference on Learning Representations, 2021.

[30] Ilya Loshchilov and Frank Hutter. Decoupled weight decay regularization. In International Conference on Learning Representations, 2018.

[31] Steph-Yves Louis, Yong Zhao, Alireza Nasiri, Xiran Wang, Yuqi Song, Fei Liu, and Jianjun Hu. Graph convolutional neural networks with global attention for improved materials property prediction. Physical Chemistry Chemical Physics, 22(32):18141–18148, 2020.

[32] Bryce Meredig, Ankit Agrawal, Scott Kirklin, James E Saal, Jeff W Doak, Alan Thompson, Kunpeng Zhang, Alok Choudhary, and Christopher Wolverton. Combinatorial screening for new materials in unconstrained composition space with machine learning. Physical Review B, 89(9):094104, 2014.

[33] Anton O Oliynyk, Erin Antono, Taylor D Sparks, Leila Ghadbeigi, Michael W Gaultois, Bryce Meredig, and Arthur Mar. High-throughput machine-learning-driven synthesis of full-heusler compounds. Chemistry of Materials, 28(20):7324–7331, 2016.

[34] Paul Raccuglia, Katherine C Elbert, Philip DF Adler, Casey Falk, Malia B Wenny, Aurelio Mollo, Matthias Zeller, Sorelle A Friedler, Joshua Schrier, and Alexander J Norquist. Machine-learning-assisted materials discovery using failed experiments. Nature, 533(7601):73–76, 2016.

[35] Rampi Ramprasad, Rohit Batra, Ghanshyam Pilania, Arun Mannodi-Kanakkithodi, and Chiho Kim. Machine learning in materials informatics: recent applications and prospects. npj Computational Materials, 3(1):1–13, 2017.

[36] Victor Garcia Satorras, Emiel Hoogeboom, Fabian Bernd Fuchs, Ingmar Posner, and Max Welling. E (n) equivariant normalizing flows. In Advances in Neural Information Processing Systems, 2021.

[37] Jonathan Schmidt, Love Pettersson, Claudio Verdozzi, Silvana Botti, and Miguel A. L. Marques. Crystal graph attention networks for the prediction of stable materials. Science Advances, 7 (49):eabi7948, 2021. doi: 10.1126/sciadv.abi7948.

[38] Kristof Schütt, Pieter-Jan Kindermans, Huziel Enoc Sauceda Felix, Stefan Chmiela, Alexandre Tkatchenko, and Klaus-Robert Müller. Schnet: A continuous-filter convolutional neural network for modeling quantum interactions. Advances in neural information processing systems, 30, 2017.

[39] Nino Shervashidze, Pascal Schweitzer, Erik Jan Van Leeuwen, Kurt Mehlhorn, and Karsten M Borgwardt. Weisfeiler-lehman graph kernels. Journal of Machine Learning Research, 12(9), 2011.

[40] Leslie N Smith and Nicholay Topin. Super-convergence: Very fast training of residual networks using large learning rates. 2018.

[41] Jonathan M Stokes, Kevin Yang, Kyle Swanson, Wengong Jin, Andres Cubillos-Ruiz, Nina M Donghia, Craig R MacNair, Shawn French, Lindsey A Carfrae, Zohar Bloom-Ackermann, et al. A deep learning approach to antibiotic discovery. Cell, 180(4):688–702, 2020.

[42] Petar Veličković, Guillem Cucurull, Arantxa Casanova, Adriana Romero, Pietro Liò, and Yoshua Bengio. Graph attention networks. In International Conference on Learning Representations, 2018.

[43] Anthony Yu-Tung Wang, Steven K Kauwe, Ryan J Murdock, and Taylor D Sparks. Compositionally restricted attention-based network for materials property predictions. Npj Computational Materials, 7(1):1–10, 2021.

[44] Zhengyang Wang, Meng Liu, Youzhi Luo, Zhao Xu, Yaochen Xie, Limei Wang, Lei Cai, Qi Qi, Zhuoning Yuan, Tianbao Yang, et al. Advanced graph and sequence neural networks for molecular property prediction and drug discovery. Bioinformatics, 38(9):2579–2586, 2022.

[45] Logan Ward, Ankit Agrawal, Alok Choudhary, and Christopher Wolverton. A general-purpose machine learning framework for predicting properties of inorganic materials. npj Computational Materials, 2(1):1–7, 2016.

[46] Zhenqin Wu, Bharath Ramsundar, Evan N Feinberg, Joseph Gomes, Caleb Geniesse, Aneesh S Pappu, Karl Leswing, and Vijay Pande. Moleculenet: a benchmark for molecular machine learning. Chemical science, 9(2):513–530, 2018.

[47] Tian Xie and Jeffrey C Grossman. Crystal graph convolutional neural networks for an accurate and interpretable prediction of material properties. Physical review letters, 120(14):145301, 2018.

[48] Tian Xie, Xiang Fu, Octavian-Eugen Ganea, Regina Barzilay, and Tommi Jaakkola. Crystal diffusion variational autoencoder for periodic material generation. iclr, 2022.

[49] Chengxuan Ying, Tianle Cai, Shengjie Luo, Shuxin Zheng, Guolin Ke, Di He, Yanming Shen, and Tie-Yan Liu. Do transformers really perform badly for graph representation? Advances in Neural Information Processing Systems, 34, 2021.

Checklist

1. For all authors...
   (a) Do the main claims made in the abstract and introduction accurately reflect the paper's contributions and scope? [Yes]
   (b) Did you describe the limitations of your work? [No]
   (c) Did you discuss any potential negative societal impacts of your work? [N/A]
   (d) Have you read the ethics review guidelines and ensured that your paper conforms to them? [Yes]
2. If you are including theoretical results...
   (a) Did you state the full set of assumptions of all theoretical results? [Yes]
   (b) Did you include complete proofs of all theoretical results? [Yes] See Appendix. A.2.
3. If you ran experiments...
   (a) Did you include the code, data, and instructions needed to reproduce the main experimental results (either in the supplemental material or as a URL)? [Yes] We have included the detailed settings of our experiments. We will publish our implementation upon acceptance.
   (b) Did you specify all the training details (e.g., data splits, hyperparameters, how they were chosen)? [Yes] See Appendix. A.3 and Appendix. A.4.
   (c) Did you report error bars (e.g., with respect to the random seed after running experiments multiple times)? [N/A] Error bars are not necessary for baseline methods and our method.
   (d) Did you include the total amount of compute and the type of resources used (e.g., type of GPUs, internal cluster, or cloud provider)? [Yes] All of these are reported in Appendix. A.3.
4. If you are using existing assets (e.g., code, data, models) or curating/releasing new assets...
   (a) If your work uses existing assets, did you cite the creators? [Yes]
   (b) Did you mention the license of the assets? [N/A]
   (c) Did you include any new assets either in the supplemental material or as a URL? [N/A]
   (d) Did you discuss whether and how consent was obtained from people whose data you're using/curating? [N/A]
   (e) Did you discuss whether the data you are using/curating contains personally identifiable information or offensive content? [N/A]
5. If you used crowdsourcing or conducted research with human subjects...
   (a) Did you include the full text of instructions given to participants and screenshots, if applicable? [N/A]
   (b) Did you describe any potential participant risks, with links to Institutional Review Board (IRB) approvals, if applicable? [N/A]
   (c) Did you include the estimated hourly wage paid to participants and the total amount spent on participant compensation? [N/A]